The Morphology and Property of HDPE in the Presence of Oscillation Pressure and Poly(ethylene terephthalate)

Xinyuan Qian, Hong Liu, Fanghui Liu, Xueqin Gao, Jie Zhang

State Key Laboratory of Polymer Materials Engineering, College of Polymer Science and Engineering, Sichuan University, Chengdu, China 610065

Received 17 October 2010; accepted 7 March 2011
DOI 10.1002/app.34499
Published online 29 July 2011 in Wiley Online Library (wileyonlinelibrary.com).

ABSTRACT: The injection-molded specimens of neat HDPE and the PET/HDPE blends were prepared by conventional injection molding (CIM) and by pressure vibration injection molding (PVIM), respectively. The effect of oscillation pressure and PET phase with different shapes on superstructure and its crystal orientation distribution of injection molded samples were characterized by differential scanning calorimetry (DSC), scanning electron microscopy (SEM), and two-dimension wide-angle X-ray diffraction techniques (2D-WAXD). Hermans' orientation functions were determined from the wide-angle X-ray diffraction patterns. With the PET particles added, the shear viscosity of blend increase and crystallization rate of HDPE phase is enhanced. For the neat HDPE samples, with the promotion from oscillation shear, the orientation parameter experienced a large increase, moreover, the PVIM can induce transverse lamellae (kebabs) twisting in growth direction. Because of the redefined flow field and nucleation effect of PET particles, the crystal orientation of blend is also increased. So the tensile strength of vibration samples enhanced and elongation at break declined. © 2011 Wiley Periodicals, Inc. J Appl Polym Sci 123: 682–690, 2012

Key words: PET/HDPE blend; crystal orientation; conventional injection molding; pressure vibration injection molding; lamellae twisting

INTRODUCTION

Blending of polymers is considered to be an advantageous and economical method to obtain products with superior performance. Morphology control of the dispersed phase is extremely important to achieve good properties for the resultant polymer blend. PET and HDPE are used extensively in packaging materials, and their annual rates of growth of production and consumption steadily increase. Combining PET and PE can yield unusual properties; the blends can be less brittle than PET and may no longer need to be dried before processing. They are generally stiffer and faster cooling than HDPE, so they can be molded and extruded with faster cycles and higher outputs.[1] And at the same time PET phase in HDPE acts as heterogeneous nuclei during nonisothermal crystallization process,[2] and hence the crystallization rate of HDPE phase is enhanced, especially when PET phase is deformed into microfibers during processing, and its effect on HDPE crystallization is considerably enhanced.[3]

In fact, the final performance of the products of polymer blend depends on the properties of the individual components as well as on the microstructure formed mainly in the processing stage. During the injection molding cycle, high shear and temperature gradient are developed in the polymer melt. From many experimental observations, it is known that in the injection-molded articles of semicrystalline polymers, the high stresses near the wall give rise to a highly oriented lamellar crystallite microstructure, the so-called skin layer. In the core region, where the stresses are relatively low, the melt is allowed to crystallize three-dimensionally to form spherulitc microstructure. As for the injection-molded samples of polymer blends, the morphology of the "skin-core" structure involves three aspects: a phase behavior hierarchy for the dispersed phase, crystalline or orientated structural hierarchy for matrix, as well as a hierarchy structure of cocontinuous phase morphology.[4]

Elongational flow injection molding is a processing method which yields high strength materials due to the self-reinforcing capability of the highly oriented fibrils.[5,6] The morphology of these oriented materials is described as that of shish-kebab fibrils.[7,8] It consists predominantly of oriented shish cores along the injection direction and laterally grown

Correspondence to: J. Zhang (zhangjie@scu.edu.cn).
Contract grant sponsor: National Natural Science Foundation of China; contract grant numbers: 50873072, 50803038.
Contract grant sponsor: Special Funds for State Key Laboratory.

stacked lamellae with the layer normals in the same direction. In comparison with elongational flow, the shear flow is often thought to be a weaker flow, not able to provide sufficient extension to the chains necessary to form the fibrillar structure. However, many experimental results suggest that this consideration is not founded. In several studies, even with the application of relatively weak shear conditions, the overall crystallization kinetics were found to change drastically, and the shish-kebab morphology was observed.[9–14] In a previous review by Keller and Kolnaar, they also argued that although the full extension of the chains in shear was unlikely, the extension of portions of the chain was still possible, which could form the basis for the shish-kebab structure.[15]

Note that the feature of pressure vibration injection molding (PVIM) is that the vibration shear stress can be imposed on polymer melt during the filling and packing stage, hence leading to a high level of molecular orientation even in the core region,[16] which is a good tool to investigate the effect of complex flow field during the practical polymer processing on the morphology as well as properties of semicrystalline polymers and their blends.

In this study, using the PVIM and PET/HDPE blend we investigated in detail the effect of the combination of shear flow and the addition of PET particles on the crystalline morphology as well as morphology distribution in injection-molded parts. Both conventional injection molding and pressure vibration injection-molding were used to prepare the samples. The effect of shear stress and PET dispersed phase with different shape on superstructure and its crystal orientation distribution of molded blend samples was investigated by means of two-dimension wide angle X-ray diffraction (2D-WAXD).

EXPERIMENT

Materials

The resins used in this study were high density PE and PET, where PET was used as the dispersed phase and PE as the matrix. HDPE (TR144) was purchased from Maoming Petroleum Chemical, China. Its melt flow rate (MFR) was 0.2 g/10 min at 190°C, exerting a force of 21.6*N*. PET pellets were supplied by UBE, Japan. Its number average molecular weight (M_n) was 2.1 $\times$ 10^4 g mol^{-1}. The rheological behavior of neat HDPE and HDPE/PET blend are shown in Figure 1, which were obtained using a capillary rheometer (GoettfertRHEOGRAPH2002) at 190°C with a capillary die of 1 mm diameter and a length to diameter (L/D)ratio of 30.

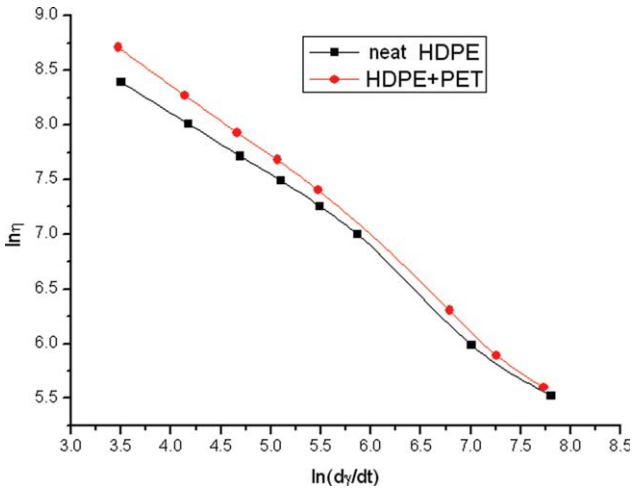

Figure 1 Shear viscosity of HDPE and HDPE/PET blend resins as a function of shear rate at 190°C. [Color figure can be viewed in the online issue, which is available at wileyonlinelibrary.com.]

Samples preparation

PET was dried for 12 h before processing under vacuum at 100°C to avoid the hydrolytic degradation, and then dry-mixed with PE in a fixed weight ratio of 15/85. The mixture was then blended in a twin-screw extruder (SHJ-25, Screw diameter-25mm, L/D ratio-44) with a temperature profile: 190, 230, 250, 260, 270, and 275°C from hopper to die. The screw speed was maintained at 100 rpm. The extrudate in the form of thread through a rod die was pelletized and dried before injection molding. Then the PET/HDPE blend was injected into the mold under PVIM. During the processing, the injection ram was driven by vibration and injection system. The injection system provides the basic pressure while vibration system provides oscillatory pressure, so a periodically changing pressure acts on the melt in the runner and mold cavity until the injection gate is frozen. A schematic representation of the melt vibration injection apparatus had been described in our previous articles.[16,17] The processing parameters were shown in Table I, which were set on the control panel. For the purpose of comparison, conventional injection molding was (CIM) carried out under static packing (without vibration) by using the same processing parameters. The samples were dumbbell-shaped, as shown in Figure 2

Characterizations

Mechanical properties

Measurement of tensile strength was performed for dumbbell specimens according to ASTM D 638-03 at room temperature of 25°C. During tensile testing, the crosshead speed was maintained at 50 mm min^{-1}.

TABLE I
The Parameters of Process

	Vibration pressure (MPa)	Vibration frequency (Hz)	Melting temperature (°C)	Injection and packing pressure (MPa)	Mould temperature (°C)
CIM	–	–	190	35	60
PVIM	45	1.25	190	35	60

Two-dimension wide-angle X-ray diffraction (2D-WAXD)

The orientation distributions across the thickness direction were characterized by the two-dimension wide-angle X-ray diffraction (2D-WAXD). The two-dimensional WAXD experiments were carried out at room temperature upon the U7B beam line in the National Synchrotron Radiation Laboratory (NSRL), University of Science and Technology of China, Hefei. The samples used were taken from the middle section of the tensile bar, which was divided into five layers from skin to the core, as shown in the Figure 2. Layer one was the surface layer and the last layer was core layer. Each layer with the thickness of 500 μm was scanned by X-ray 2D-WAXD measurements. The wavelength used was 0.1548 nm, the sample-to-detector distance was 185 mm, and the direction of the X-ray beam was perpendicular to MD-TD (the molding direction-transverse direction) plane. The orientations of the crystals of HDPE was calculated using the Herman's orientation parameter, which was defined as

$$\langle P_2(\cos\phi)\rangle = (3\langle\cos^2\varphi\rangle - 1)/2 \tag{1}$$

where $\cos^2\varphi$ is an orientation factor defined as

$$\left(\cos^2\phi\right) = \frac{\int_0^{\frac{\pi}{2}} I(\phi)\sin\phi\cos^2\phi d\phi}{\int_0^{\frac{\pi}{2}} I(\phi)\sin\phi d\phi} \tag{2}$$

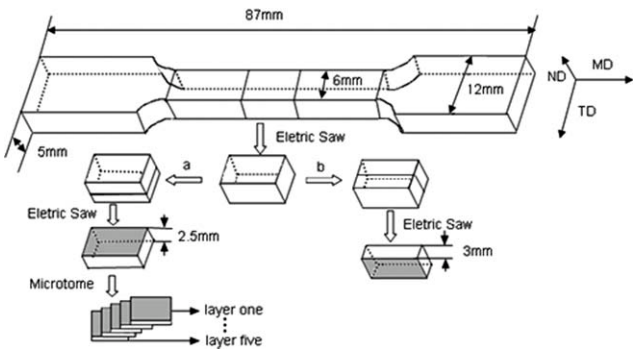

Figure 2 The sketch of part obtained by PVIM, CIM, and the schematic of position of the sample for test. a: prepared for 2D-WAXD test; b: prepared for SEM test.

where $I(\varphi)$ is the scattering intensity at φ. The orientation parameter has a value of unity when all the crystals are oriented with their *c* axes parallel to the reference direction (i.e., the flow direction), a value of -0.5 when all the *c* axes are perpendicular to the reference direction, and a value of 0 with totally random orientation. For our samples, the orientation parameter was calculated mathematically using Picken's method of (110) reflection of WAXD for HDPE.[18]

Scanning electron microscopy (SEM)

For the SEM observation, the samples were ground to the middle MD-ND plane and polished, then etched for a certain time in an etchant consisting of a 3% w/v solution of potassium permanganate dissolved in the sulfuric and dry *ortho*-phosphoric acids mixed solution, and then washed with 30% hydrogen peroxide and distilled water. The samples were gold sputtered before the observation.

Differential scanning calorimetry (DSC)

The thermal properties of the neat HDPE and HDPE/PET blend were determined by a Netzsch DSC 204 differential scanning calorimeter with the following standard procedure: the samples (about 5–8 mg) were melted at 200°C for 5 min to eliminate any thermal history in the material, then were cooled to 40°C at a predetermined constant rate of -20°C min^{-1} for nonisothermal crystallizing. The experiments were carried out in nitrogen atmosphere.

RESULTS AND DISCUSSION

Tensile strength and elongation at break of different samples are shown in the Table II. Comparing with the CIM samples, the tensile strength of PVIM samples increase, but the elongation at break reduce. For example, the increment of tensile strength of neat HDPE is 9.3%, from 30.2 MPa of conventional injection-molded sample to 33.1 MPa of pressure vibration injection-molded one, which is higher than that of PET/HDPE blend samples (8.5%), from 32.2 to 35.0 MPa. Comparing with the neat sample, the tensile strength of blend also increases, the maximal increment is 15.75%, from 30.28 MPa of neat sample to 35.0 MPa of PET/HDPE blends, as for the reason we will discuss later.

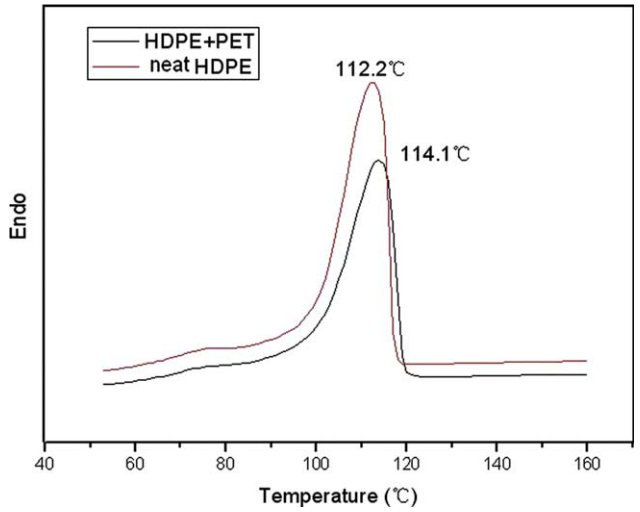

Figure 3 DSC thermograms for crystallization of HDPE phase of neat HDPE and HDPE/PET PVIM samples. [Color figure can be viewed in the online issue, which is available at wileyonlinelibrary.com.]

The crystallization exotherms of PVIM neat HDPE sample and PVIM HDPE/PET blend sample at a predetermined cooling rate of $-20°C\ min^{-1}$ are presented in Figure 3. Based on these curves, some useful parameters, such as onset and peak or maximum crystallization rate temperatures (T_o and T_p, respectively), undercooling temperature ($\triangle T_c$), maximum crystallization time (t_{max}, time required to crystallize from T_0 to T_p) and half crystallization time ($t_{1/2}$) can be obtained for describing the nonisothermal crystallization behavior of these materials studied. As shown in Table III, at a cooling rate of $-20°C\ min^{-1}$, for HDPE/PET blends, T_o and T_p are higher, $\triangle T_c$, t_{max}, and $t_{1/2}$ are lower than those for neat HDPE. On the basis of these results, it implies that HDPE/PET blend crystallizes faster than does neat HDPE. In other words, PET phase in HDPE acts as heterogeneous nuclei during nonisothermal crystallization process, and hence the crystallization rate of HDPE phase is enhanced.

The relative crystallinity (X(T)) is expressed as

$$X(t) = \int_{T_0}^{T} \left(\frac{dH}{dt}\right) \Big/ \int_{T_0}^{T_2} \left(\frac{dH}{dt}\right) dt \qquad (3)$$

where T_0 and T_2 are the onset and end of crystallization temperatures, respectively; dH/dt is the heat-evolution rate. Figure 4(a) shows the relative crystallinity, $X(t)$, as a function of temperature for neat HDPE and HDPE/PET blend at a predetermined cooling rate of $-20°C\ min^{-1}$. All these curves have the same sigmoidal shape, indicating the lag effect of cooling rate upon crystallization. Using the following expression, $t = (T_0 - T)/R$ (where T is the temperature at crystallization time t and R is the cooling rate), the abscissa of temperature in Figure 4(a) can be transformed into a time scale as shown in Figure 4(b). These curves show that at the same crystallization time, the relative crystallinity of HDPE/PET blend is higher than that of neat HDPE.

TABLE II
The Tensile Strength and Elongation at Break of Four Samples

	Tensile strength (MPa)	Elongation at break (%)
CIM neat HDPE sample	30.2 ± 0.8	73.22
PVIM neat HDPE sample	33.1 ± 1.0	38.26
CIM PET/HDPE blend sample	32.2 ± 1.1	24.42
PVIM PET/HDPE blend sample	35.0 ± 0.9	19.44

To observe the distribution of the PET particles phase, etching technique and field emission SEM are employed. Figure 5 shows representative SEM micrographs of HDPE/PET sample molded by CIM and PVIM. Because the disperse PET particles is fully etched out, its disperse morphology in different regions can be represented by the voids in the micrographs. As the injection temperature (190°C) is below the melting point of PET, HDPE melts while PET stays in solid state. The PET particles are spheres or ellipsoids and uniformly dispersed in the HDPE matrix no matter in the shear region and in the core region [as shown in Fig. 5(a,b)].

For immiscible polymer blends, under both strong stress field and nonisothermal temperature profile, the deformable minor phase can be deformed *in situ* into a variety of morphological structures such as spheres, ellipsoids, fibers, and plates.[19–22] So the situation during the pressure vibration injection molding of HDPE/PET blend is much more complicated. Because HDPE melt and PET particles all experienced a continuous oscillation flow during packing, the morphological structures of minor phase were elongated ellipsoids in the shear regions which means that the PET particles were stretched by the shear flow along the flow direction. However, the morphology of PET phase kept the original

TABLE III
Thermal Properties of HDPE Phase in Neat HDPE and HDPE/PET Vibration Samples Obtained from DSC Studies

Sample	T_0 (°C)	T_P (°C)	T_m (°C)	t_{max} (s)	$t_{1/2}$ (s)	ΔT_c (°C)
PVIM neat HDPE	120.1	112.2	129.4	23.7	42.2	17.2
PVIM HDPE/PET	121.1	114.1	128.2	21.0	36.1	14.1

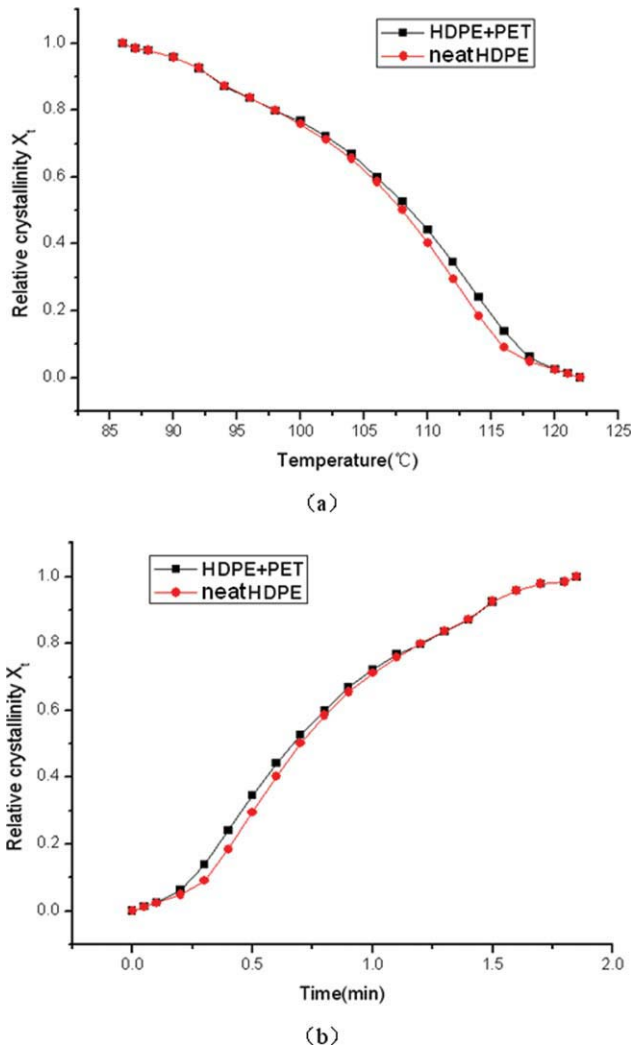

Figure 4 The relative crystallinity of HDPE phase (a) The variation of relative crystallinity of HDPE phase with temperature during crystallization for neat HDPE and HDPE/PET PVIM samples, (b) The variation of relative crystallinity of HDPE phase with time during crystallization for neat HDPE and HDPE/PET PVIM samples. [Color figure can be viewed in the online issue, which is available at wileyonlinelibrary.com.]

structure: spheres or ellipsoids in the core region [as shown in Fig. 5(c,d)].

Figure 6 shows the 2D-WAXD patterns of the four samples at different distances from their skin. In the CIM neat sample, the full Debye rings or near-isotropic rings appears nearly in the whole sample except the layer one and two, which reveals the absence of pronounced orientation. The Debye rings of other three samples are arcing in the equatorial plane, which means obvious orientation. There exist some obvious reflections in the equator, which can be indexed as the (110) at $2\theta = 21.6°$, (200) at $2\theta = 23.1°$. However, four (110) reflections in the form of arcs at the off-axis direction and two (200) reflections in the meridian are seen in intermediary layers of PVIM neat HDPE samples in Figure 6(b). The appearance of four-arc off-axis (110) reflections and two-arc meridional (200) reflections is an indication of twisted lamellae.

Figure 7 shows the (110) intensity distribution along the azimuthal angle between 0° and 360° (azimuthal angle = 0° and 360° represent the meridional axis, azimuthal angle = 90° and 270° represent the equatorial axial). Characteristic peaks of azimuthal angle mainly appear in the equatorial axial, except that in the intermediary region of PVIM neat sample four peaks generate in the off-axis direction, which is the same as the result of images. Meanwhile the peaks are sharper in the skin region and intermediary region than that of core region, which illustrate a higher orientation in the skin and intermediary layers. To quantitatively analyze the orientation of each layer, the orientation parameters at different distances were calculated from the (110) intensity distribution along the azimuthal angle using eqs. (1) and (2), which are presented in Figure 8. For the neat HDPE sample, the typical skin core structure across the direction of thickness exists in the conventional injection-molded sample. The orientation parameter P_2 is around 0.57 in the skin layer and around 0 in the core region. For the PET/HDPE blend, the hierarchy structure across the thickness direction also appears. The maximum of the orientation parameter is about 0.54 in the skin layer and orientation parameter is just about 0.15 in the core region, and the difference of orientation parameters (0.39) is lower than that of the neat sample (0.57). The orientation parameters of blend sample in the first two layers are lower than those of neat sample, but the situation is opposite in the subsequent three layers.

To enhance the orientation of HDPE crystals, the pressure vibration injection molding (PVIM) is employed for both neat HDPE and HDPE/PET blend. The orientation parameters were extracted and were plotted in Figure 8. For neat HDPE sample, the degree of crystal orientation for each layer has been enhanced due to the high oscillation shear force imposed on HDPE melt during the injection molding. However, it can not completely eliminate the hierarchical structure of neat HDPE sample, the difference of orientation parameter is 0.55. For the PET/HDPE blend sample, in the synergistic effect of oscillation flow and confined flow, the orientation parameters in the all regions of blend sample are higher than those of PVIM neat HDPE sample. Whereas the difference of orientation parameters is 0.58 between layer one (0.80) and core layer (0.22), which is almost identical to that of PVIM neat HDPE sample.

Under the nonisothermal condition, the orientation of crystals is determined by the shear rate, shear

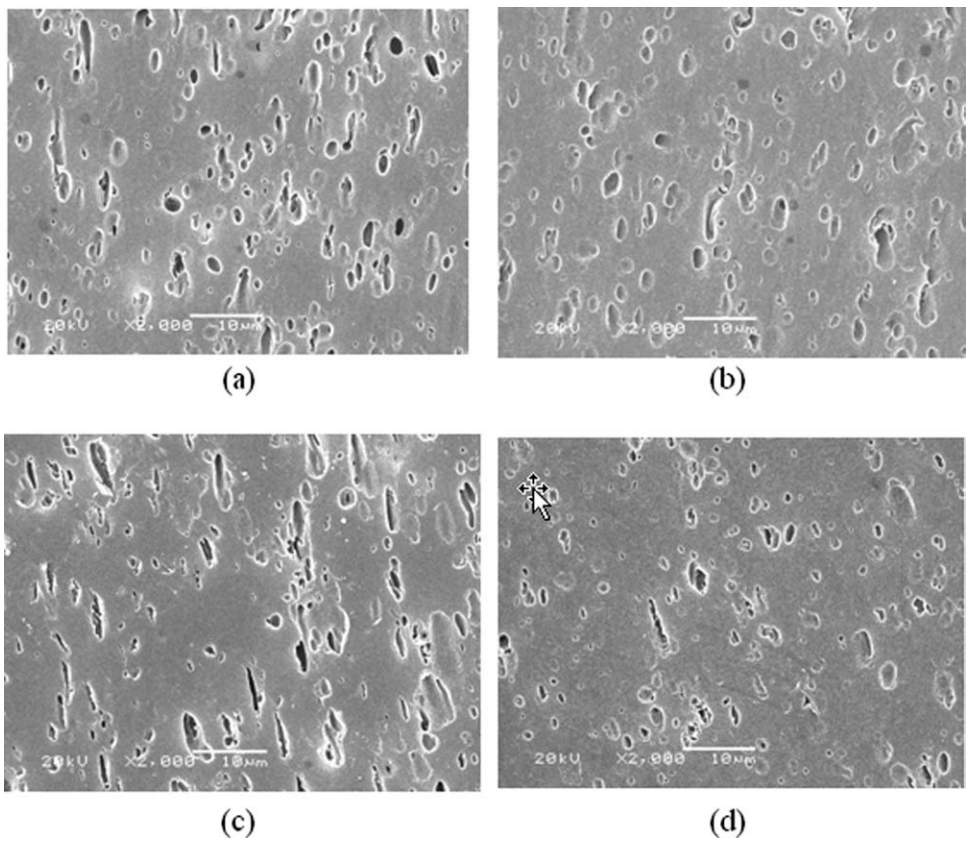

Figure 5 The SEM microphotographs in the different region of PET/HDPE blend. (a) and (c): skin region; (b) and (d): the core region; (a) and (b): CIM sample; (c) and (d): PVIM sample. The flow direction is vertical.

stress, and cooling rate. It is well-established that the orientation of polymer molecules is a result of the competition between shear-induced orientation and chain stretching and subsequent relaxations.[23] Higher stress lead to a higher orientation of molecular chains, while a faster cooling rate slows down the relaxation or even freezes the orientation by the kick-in of crystallization. Considering these general rules in mind, let us first look at the conventional injection molding. When neat HDPE melt was injected into mold, the skin layer was immediately cooled by cold mold wall, leading to a high shear stress. A combination of the high shear stress and low temperature generated a high orientation of crystals at skin layer (see Figure 8). Because of temperature gradient from skin to core, a delay of crystallization was expected in the regions away from skin, which give the different time windows for molecules to relax. This can explain the nearly linear decrease of orientation parameter from skin to core.

The same mechanisms also happened during pressure vibration injection molding. During processing, the HDPE melt suffered the shear force continuously until it finished crystallization and solidification, which resulted in an increase of orientation parameters of HDPE crystals in all regions. With the promotion from oscillation shear, the orientation parameters in all regions of neat HDPE experienced a large increase, nevertheless, the orientation parameters in the core region was still lower than that at skin and intermediary regions, and a heterogeneous structure existed.

During the flow, the stretch chains can crystallize into shish, while the coiled chain can be adsorb onto the shish and transform into the lamellae (kebab).[24] The degree of stretch, caused by the strength of the flow, can affect not only the number of nucleating threads (shish) but also the configuration of the transversely growing lamellae (kebabs). In weaker orientating flows, fewer and hence more widely spaced shish are formed, and the transverse lamellae (kebabs) show twisting in growth direction due to chain tilting, such as is usual in (polyethylene) spherulites.[15,25,26]

On the basis of our WAXD data, we conclude that lamellae in neat HDPE prepared by PVIM eventually develop into a twisted structure, which is verified by the unique appearance of the (200) reflection. For example, in Figure 6(b), a pair of (200) reflections are seen in the meridional direction. If the lamellar structure is flat, the *c*-axis of the crystals should be aligned parallel to the flow direction and the *b*-axis should be perpendicular to the flow direction. This would result in the appearance of two

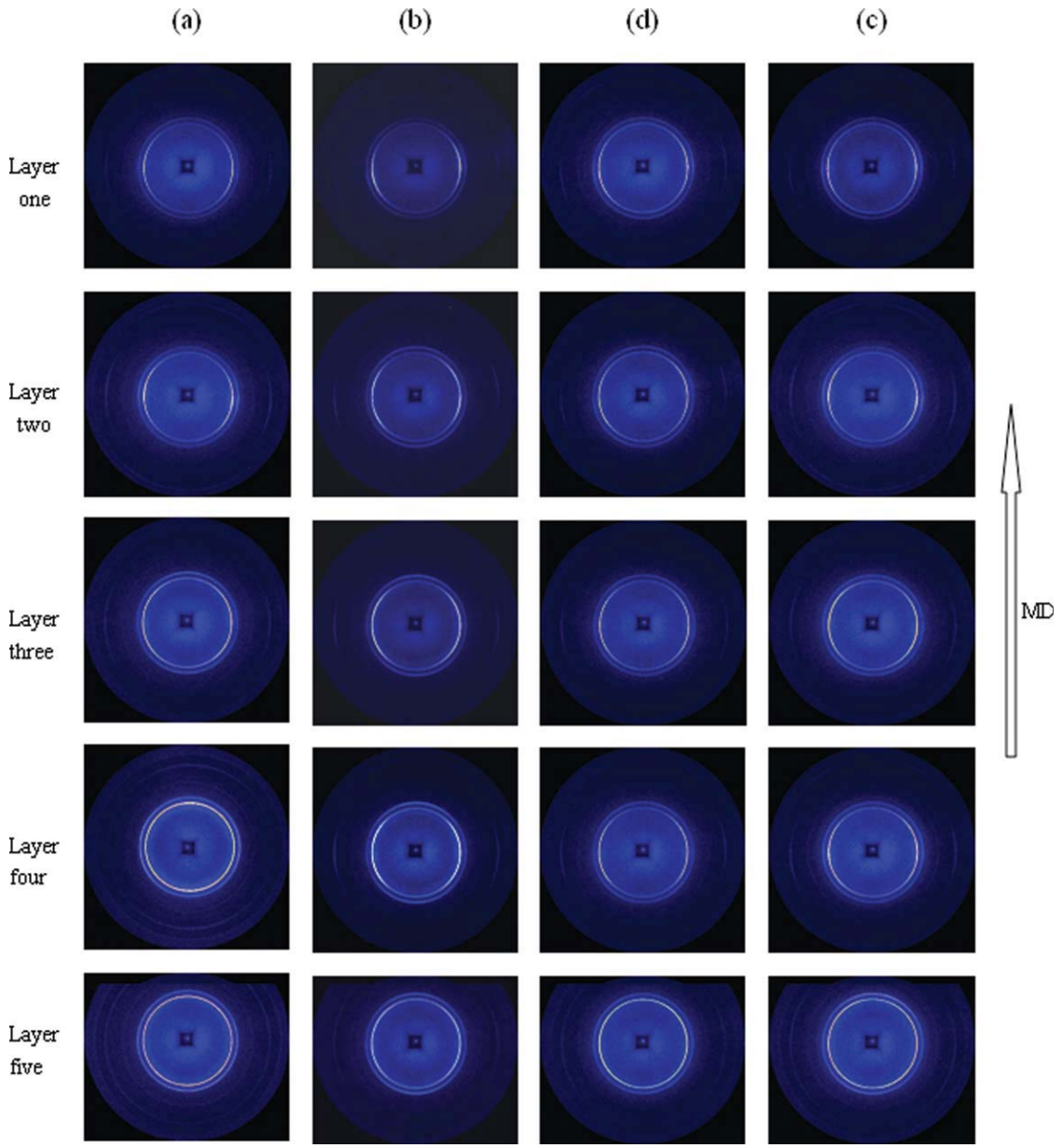

Figure 6 The 2D-WAXD patterns of four samples. (a): CIM neat HDPE sample; (b): PVIM neat HDPE sample; (c): CIM PET/HDPE sample; (d): PVIM PET/HDPE sample. [Color figure can be viewed in the online issue, which is available at wileyonlinelibrary.com.]

(200) reflections on the equator. If twisted lamellae are developed during growth, as previously reported by Keller and Schultz in flow-induced crystallization of PE,[15,26] the crystal *a*- and *c*-axes would rotate around the *b*-axis, resulting in the changes of the (200) reflection from equatorial alignment to meridional alignment. The twisted lamellar structure is also consistent with the appearance of four (110) reflection peaks at the off-axis positions.

With the same injection pressure as for neat HDPE, the HDPE melt including PET particles had a lower flow rate to fill the mold due to higher viscosity. Thus, a lower shear rate was imposed at the skin layer, which brought down the orientation parameter (0.54). In the core region, the situation was opposite. On one hand, the PET particles that split the space of HDPE melt movement played effectively as a solid wall and redistributed the flow field, and hence HDPE molecules experienced confined flow in the surface of the PET particles. Compared to neat HDPE melt, the local shear stress in the core region of HDPE/PET blend was higher, which led to higher orientation of molecular chains. On the other hand, PET particles served as nucleation agent and nucleation enhancer under flow condition.

The situation during pressure vibration injection molding of HDPE/PET blends was much more

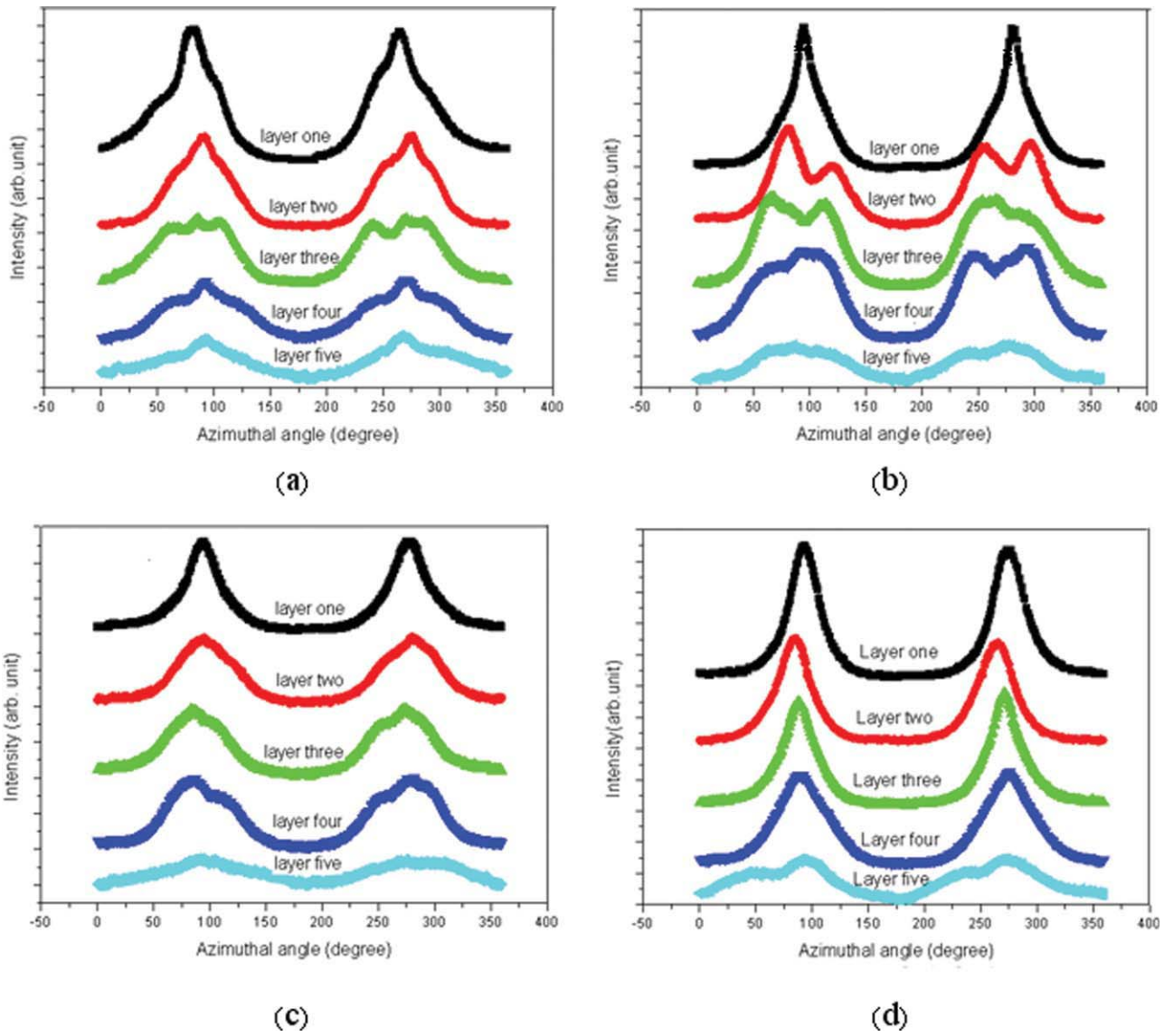

Figure 7 The intensity distribution of (110) along azimuthal angle. (a): CIM neat HDPE sample; (b): PVIM neat HDPE sample; (c): CIM PET/HDPE sample; (d): PVIM PET/HDPE sample. [Color figure can be viewed in the online issue, which is available at wileyonlinelibrary.com.]

complicated than that in pure HDPE melt. Here not only did HDPE melt experience a continuous oscillation flow during packing, but also the PET particles changed its configuration continuously. When the HDPE matrix melt pushed PET particles into the mold, the stretched PET particles had some degree of preferred orientation along the flow direction. The preferred orientation of PET particles indicated a relative movement and stress between melt and solid particles. In the synergistic effect of oscillation flow and confined flow, the orientation parameters in all the regions of blend sample increased.

The orientation parameters of PVIM neat HDPE samples increase comparing with those of the CIM samples; therefore the tensile strength of vibration samples increase and the elongation at break reduce. As for the tensile strength of PET/HDPE blends also increase comparing with that of neat HDPE, the reason is as follows: first HDPE melt suffered a shear force in the vicinity of PET particles due to the relative flow rate of two components, which induced alignment of HDPE molecules along the particle axes. Second the HDPE had a large thermal contraction while the PET particles had almost no shrinkage after cooling; the HDPE matrix was coated tightly on the PET particles in the samples. Moreover, it was the frictional force in the interfaces between PET and PE that transferred the stress to the PET particles, hence giving rise to the reinforcement of PE by PET particles.

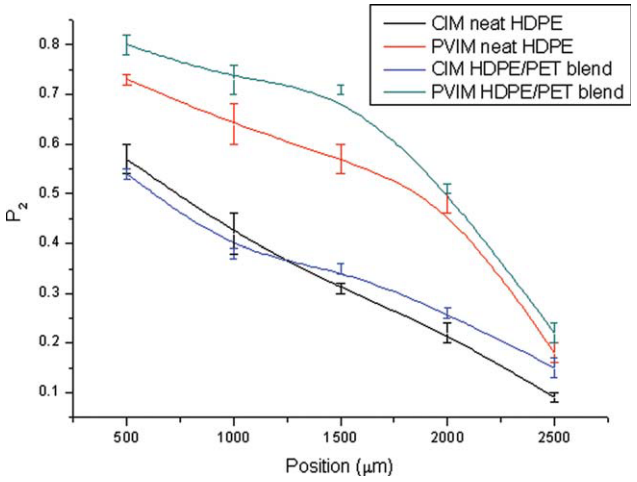

Figure 8 The orientation parameter of four samples. [Color figure can be viewed in the online issue, which is available at wileyonlinelibrary.com.]

CONCLUSIONS

The effect of shear stress and PET dispersed phase with different shape on superstructure was investigated by means of wide angle X-ray diffraction (WAXD), scanning electron microscope (SEM), and differential scanning calorimetry (DSC). Hermans' orientation functions were determined from the wide-angle X-ray diffraction patterns. As the heterogeneous nuclei of HDPE during nonisothermal crystallization process, PET particles can enhance the crystallization rate of HDPE phase and increase the shear viscosity of blend. With the promotion from oscillation shear, the orientation parameter of neat HDPE experience a large increase, so the tensile strength of PVIM sample is larger than that of the CIM sample. The degree of stretch, caused by the strength of the oscillation pressure flow, can affect not only the number of nucleating threads (shish) but also the configuration of the transversely growing lamellae (kebabs). The transverse lamellae (kebabs) of the PVIM neat HDPE sample show twisting in growth direction due to the crystal *a*- and *c*-axes rotate around the *b*-axis. The crystal orientation of blend also increases; this is attributed by the redefined flow field and nucleation effect of PET particles. And at the same time HDPE melt suffers a shear force in the vicinity of PET particles, which induces alignment of HDPE molecules along the particle axes. So the tensile strength of blend increases though they are immiscible.

The authors are indebted to the National Synchrotron Radiation Laboratory (NSRL) in University of Science and Technology of China and Prof. Guoqiang Pan (NSRL) for their help in synchrotron WAXD experiment.

References

1. Akovali, G.; Bernardo, C. A. Kluwer Academic Publishers: Norwell, 1998.
2. Li, Z. M.; Yang, W. J Polym Sci B Polym Phys 2004, 42, 374.
3. Evstatiev, M.; Fakirov, S.; Covas, J. A.; Cunha, A. M. ibid 2002, 42, 826.
4. Zhong G. J.; Li, Z. M. Polym Eng Sci 2005, 45, 1655.
5. Bayer, R. K.; Eliah, A. E.; Seferis, J. C. Polym Eng Rev 1984, 201, 4.
6. Ehrenstein, G. W.; Maertin, C. Kunststoffe 1985, 75, 105.
7. Martinez-Salazar, J.; Bayer, R. K. Coll Polym Sci 1989, 267, 409.
8. Ania, F.; Bayer, R. K.; Tschmel, A.; Michler, H. G. J Mater Sci 1996, 31, 4199.
9. Somani, R. H.; Yang, L.; Hsiao, B. S.; Agarwal, P. K. Macromolecules 2002, 35, 9096.
10. Agarwal, P. K.; Somani, R. H.; Weng, W.; Mehta, A. Macromolecules 2003, 36, 5226.
11. Hobbs, J. K.; Miles, M. J. Macromolecules 2001, 34, 353.
12. Hobbs, J. K.; Humphris, A. D. L.; Miles, M. J. Macromolecules 2001, 34, 5508.
13. Kalay, G.; Zhong, Z. P.; Allan, P.; Bevis, M. J. Polymer 1996, 37 2077.
14. Li, Y. B.; Liao, Y. H.; Yuan, Y. J Polym Sci B Polym Phys 2005, 43, 13.
15. Keller, A.; Kolnaar, H. W. Mater Sci Technol 1997, 18, 189.
16. Zhang, J.; Shen, K. J Appl Polym Sci 2005, 96, 818.
17. Zhang, J.; Shen, K. J Polym Sci B Polym Phys 2004, 42, 2385.
18. Picken, S. J.; Aerts, J.; Visser, R.; Northolt, M. G. Macromolecules 1990, 23, 3849.
19. Favis, B. D. In Polymer Blends: Formulation; Paul, D. R.; Bucknall, C. D., Eds.; New York: Wiley, 2000; Vol.1, p 502.
20. Favis, B. D.; Chalifoux, J. P. Polymer 1988, 29, 1761.
21. Hsiung, C. M.; Cakmak, M. Polymer 1996, 37, 4555.
22. Evstatiev, M.; Fakirov, S.; Krasteva, B. Polym Eng Sci 2002, 42, 826.
23. Doi, M.; Edwards, S. F. The Theory of Polymer Dynamics; Clarendon: Oxford, UK, 1986.
24. Dukovski, I.; Muthukumar, M. J Chem Phys 2003, 118, 6648.
25. Keller, A.; Machin, M. J. J Macromol Sci B 1967, 1, 41.
26. Nadkarni, V. M.; Schultz, J. M. J Polym Sci Polym Phys Ed 1977, 15, 2151.